

2015

Winter Vertical Distributions of Antarctic Krill as Seen Through a New Stereo Camera System

Mary Kane
University of Rhode Island, mkkane@uri.edu

Follow this and additional works at: <https://digitalcommons.uri.edu/theses>

Terms of Use

All rights reserved under copyright.

Recommended Citation

Kane, Mary, "Winter Vertical Distributions of Antarctic Krill as Seen Through a New Stereo Camera System" (2015). *Open Access Master's Theses*. Paper 592.
<https://digitalcommons.uri.edu/theses/592>

This Thesis is brought to you by the University of Rhode Island. It has been accepted for inclusion in Open Access Master's Theses by an authorized administrator of DigitalCommons@URI. For more information, please contact digitalcommons-group@uri.edu. For permission to reuse copyrighted content, contact the author directly.

WINTER VERTICAL DISTRIBUTIONS OF ANTARCTIC KRILL AS SEEN
THROUGH A NEW STEREO CAMERA SYSTEM

BY
MARY KANE

A THESIS SUBMITTED IN PARTIAL FULFILLMENT OF THE
REQUIREMENTS FOR THE DEGREE OF
MASTER OF SCIENCE
IN
OCEANOGRAPHY

UNIVERSITY OF RHODE ISLAND

2015

MASTER OF SCIENCE IN OCEANOGRAPHY

OF

MARY KANE

APPROVED:

Thesis Committee:

Major Professor:

Susanne Menden-Deuer

Christopher Roman

Graham Forrester

Nasser H. Zawia

DEAN OF THE GRADUATE SCHOOL

UNIVERSITY OF RHODE ISLAND

2015

Abstract:

A new stereo camera system, encompassing a Sonde, acoustic Doppler current profiler (ADCP), and high-resolution-imaging cameras, was developed to improve our understanding of *in situ* Antarctic krill behaviors and distribution. Krill were observed on 18 deployments in 3 bays in the Western Antarctic Peninsula from May-June 2013. Observation conditions varied, including time of day, clear to stormy surface conditions, temperatures (-1.2°C to 0.8°C) and salinities (33.5ppt to 34.8ppt). Krill were observed in 61% of profiles. Krill distributions were found in two distinct profiles with regards to where highest abundances occurred: Type I profiles had maxima in the middle of the water column (200 to 350 meters), and Type II profiles had the greatest abundances at the bottom of the water column (200 to 800 meters). Occurrence of Type I and Type II profiles was strongly linked with time of day: Type I during dark and Type II during light periods. Krill were never observed shallower than 100m, indicating that krill reside deeper in the water column during the winter period.

Acknowledgements:

I would like to thank my major professor Susanne Menden-Deuer for her amazing mentorship, infinite patience, and the attentiveness she has given me in support of my work. This thesis was greatly improved by the critical review of Dr. S. Menden-Deuer, Dr. C. Roman, Dr. G. Forrester, Dr. B. Jenkins, and F. Morrison. Thank you to: Dr. G. Ingles, David Casagrande, Ian Vaughn, and Regina Yopak for their insight into and work with the krill camera system, and my lab mates Amanda Montalbano, Françoise Morrison, Mike Fong, and Sean Anderson for giving me critical feedback on this work. In addition, thank you to Captain John Souza and the crew of the RVIB Nathaniel B. Palmer, Drs. E. Durbin, T. Rynearson, M. Zhou, S. Menden-Deuer, and C. Roman, the science staff from the United States Antarctic Program, and all the volunteers and participants of the Seasonal Trophic Roles of *Euphausia superba* cruises. Funding for this project was provided to Drs. E. Durbin, T. Rynearson, M. Zhou, S. Menden-Deuer, and C. Roman by the National Science Foundation award no. 1142107 for the Seasonal Trophic Roles of *Euphausia superba* project.

I also want to thank all my friends and family for their support and advice on this project.

Preface:

This thesis is written in manuscript style rather than using the traditional segregation of the thesis into chapters. The manuscript text is written in the formatting style appropriate for submission to the Journal of Plankton Research, and is followed by an appendix containing detailed, ancillary information regarding the image processing methodology and the analysis techniques used.

TABLE OF CONTENTS

ABSTRACT	ii
ACKNOWLEDGEMENTS	iii
PREFACE	iv
TABLE OF CONTENTS	v
LIST OF TABLES	vii
LIST OF FIGURES	viii
MANUSCRIPT I	1
CHAPTER 1	2
INTRODUCTION	2
CHAPTER 2	6
METHODS	6
CHAPTER 3	12
RESULTS	12
CHAPTER 4	15
DISCUSSION	15
FIGURES AND TABLES	22
APPENDIX	31

REFERENCES..... 42

LIST OF TABLES:

TABLE	PAGE
Table 1. Deployment Number, Date, Time, Lat., Long, and Location	22
Table 2. Results of Model II Regression	23
Table A.1. Details of Test Horizon Images	31

LIST OF FIGURES:

FIGURES	PAGE
Figure 1. Particles Identified as Krill by Algorithm to Visual Count of Krill	24
Figure 2. Comparison of Accuracy and Yield of Algorithm Parameter Values	25
Figure 3. Salinity and Temperature Profiles	27
Figure 4. Vertical Krill Profiles	28
Figure 5. PAR at Time of Deployment to Relative Depth of Max Krill Abundance	29
Figure 6. Changes in Vertical Distribution of Krill Over Consecutive Dives.....	30
Figure A.2. Filter 1 Model II Regression Results	32
Figure A.3. Filter 2 Model II Regression Results	33
Figure A.4. Filter 3 Model II Regression Results	34
Figure A.5. Number of Krill to Number of Blobs	35
Figure A.6. Percentage Composition of Objects Correctly Identified as Krill – Aspect Ratio	36
Figure A.7. Percentage of Objects Identified as Krill – Aspect Ratio	37
Figure A.8. Percentage Composition of Objects Correctly Identified as Krill – Area	38
Figure A.9. Percentage of Objects Identified as Krill – Area	39
Figure A.11. Covariance Coefficient of Krill Seen Over Time	41

MANUSCRIPT

Winter Vertical Distributions of Antarctic Krill as seen through a New Stereo Camera System

Mary K. Kane¹, Regina Yopak², David S. Casagrande², Chris Roman^{1,2}, and Susanne
Menden-Deuer¹

¹Graduate School of Oceanography, University of Rhode Island, Narragansett, RI, USA

²School of Engineering, University of Rhode Island, Narragansett, RI, USA

This manuscript is formatted for the anticipated publication in the scientific journal
Journal of Plankton Research

Keywords: Antarctic krill, vertical distribution, winter, stereo camera system, *in situ*

Introduction:

The Antarctic krill *Euphausia superba* plays an important role in the transfer of carbon between primary producers of organic carbon and larger organisms (Quentin and Ross 1991; Nicol 2006; Nicol and Brierley, 2010; Saba *et al.* 2014). In addition to feeding some of the largest animals on the planet, the krill fishery is the largest and most economically important fishery in the Southern Ocean (Nicol 2006; Brierley 2008; Atkinson *et al.* 2009; Atkinson *et al.* 2012a). Antarctic krill are also important in the cycling of carbon in the global carbon cycle in the Southern Ocean (Atkinson *et al.* 2012b).

It has been traditionally assumed krill live in the upper portions of the water column. There have been many *in situ* studies of krill swarms in the upper 400 m of the Southern Ocean using ship sonar, Acoustic Doppler current profilers (ADCPs), and net trawls, such as MOC-NESS and Tucker trawls. The majority of krill profiling studies have been conducted in austral late spring, summer, and early fall (Lascara *et al.* 1999; Zhou and Dorland 2004; Nicol 2006; Nicol and Brierley 2010; Atkinson *et al.* 2012a). These studies have shown krill distributions vary horizontally and vertically throughout the Southern Ocean. Krill horizontal distributions are strongly influenced by physical environmental parameters, such as advection, the Southern Ocean gyres, the Antarctic Circumpolar Current (ACC), and sea-ice cover (Atkinson *et al.* 2012a, references therein). Changes in krill vertical distributions, which occur on a daily basis, are also a well-documented phenomenon. These changes are known as diel vertical migrations and are attributed to predator-avoidance behavior; krill avoid sight predators during the day by remaining at depth and come up at night to feed (Lascara *et al.* 1999; Nicol 2006;

Atkinson *et al.* 2012a). Additionally, many studies have also shown the deviations of diel vertical migration patterns of Antarctic krill; under varying abiotic and biotic conditions, such as increased predation or strong currents, krill diel vertical migration may be minimized or not occur at all (Zhou *et al.* 1994; Godlewska 1996; Lascara *et al.* 1999; De Robertis 2002; Zhou and Dorland 2004; Cresswell *et al.* 2009). Even with a century of research on krill horizontal and vertical distributions, the majority of what is known of krill distributions is only within a limited portion of their habitat.

Recently, it was discovered that krill have a much more extensive vertical habitat than previously supposed. Krill are capable of moving through the water column to interact with the benthos in depths up to 3500 m (Clarke and Tyler 2008). Furthermore, Schmidt *et al.* (2011) showed krill likely used the full extent of the water column and interact with the benthos on a regular basis, suggesting up to 20% of krill biomass may be regularly found at depths greater than 200 m during the summer (Schmidt *et al.* 2011). Unfortunately, there are few *in situ* studies of krill vertical distributions at depths greater than 200 m or how krill interact with the benthos, largely due to methodological limitations (Atkinson *et al.* 2012a). Ship sonar sampling systems are not effective in observing krill below 500m depth, and the shipboard abundance estimates of krill obtained by acoustic data can drastically change depending on the scattering strength model used (Atkinson *et al.* 2012a, references therein). Trawls may enable the determination of abundances at these depths but are invasive and may not reflect what is present in the water column (Wiebe *et al.* 2004; Atkinson *et al.* 2012a). Understanding the vertical distributions and movement of krill throughout the water column will provide insight into how krill contribute to benthic-pelagic coupling and nutrient transport

pathways in the Southern Ocean, such as reintroducing iron from benthic sources into surface waters (Schmidt *et al.* 2011).

Due to sampling challenges in the Antarctic winter, there are few winter studies on *in situ* krill distribution and behavior in winter. It is not well understood how *E. superba* is capable of winter survival in such a harsh environment (Atkinson *et al.* 2002). Krill are typically thought of as feeding on phytoplankton either in the water column or under the sea ice (Marschall 1988; Nicol 2006; Saba *et al.* 2014). However, there is limited phytoplankton presence or growth during the austral winter (Le Fèvre *et al.* 1998). As such, there are two hypothesized overwintering strategies of *E. superba*: feeding and non-feeding (Teschke *et al.* 2007). Non-feeding strategies include the utilization of fat storages (Hagen *et al.* 1996), shrinking reproductive organs and size to obtain more lipids and proteins to metabolize (Ikeda and Dixon 1982; Hagen *et al.* 1996), and a decrease in metabolic rates during winter to conserve energy (Kawaguchi *et al.* 1986; Quentin and Ross 1991; Torres *et al.* 1994). The feeding strategy involves *E. superba* utilizing other food sources. Krill do not feed exclusively on phytoplankton; they are capable of feeding on detritus in the water column, smaller zooplankton, and even other krill (Atkinson *et al.* 2002; Clarke and Tyler 2008; Schmidt *et al.* 2011; Atkinson *et al.* 2012b; Cleary *et al.* 2012). Studying winter vertical distributions of *E. superba* enables a better understanding of how these strategies contribute to krill survival.

Studying *in situ* individual krill behavior has been hampered by a lack of appropriate technologies available (Nicol and Brierley 2010). Camera systems are becoming much more common instruments when observing marine environments and organism behaviors. Cameras, such as the Video Plankton Recorder, are used in

identifying phytoplankton and zooplankton species (Davis *et al.* 2004; Ashjian *et al.* 2008). Collected images are often used in corroboration with acoustic data to determine the abundance, distribution, and biomass of large swarms of organisms (Benfield *et al.* 1998). Cameras are also used to qualitatively observe krill behavior at different depths and in response to nets (Clarke and Tyler 2008; Kawaguchi *et al.* 2011). Stereoscopic camera systems are also more commonly used as observational tools because they provide a way to calculate three-dimensional movement patterns of various organisms, from microscopic phytoplankton to larger organisms like Antarctic krill (Menden-Deuer and Grünbaum 2006; Letessier *et al.* 2013).

We created a stereoscopic camera system designed to observe and quantify Antarctic krill movement, including speed, direction, turning rates, and orientation of the krill. Here we describe the methods utilized to process and analyze the images collected from the camera system, as well as the vertical distributions of visible krill during the austral winter.

Methods:

2.1 Data Collection

Between May 19th and June 6th 2013, 43 camera deployments were conducted in 3 bays in the Western Antarctic Peninsula: Wilhelmina Bay, Andvord Bay, and Flanders Bay (Table 1). Two Manta G-145B NIR cameras with Fuji HF9HA-1B lenses were used in 2000 meter pressure housings (Deep Sea Power and Light) on a 2 meter long sled. The camera axes were mounted parallel with calibrated distance between optical centers of the imaging sensors was 104 mm. With the exception of two deployments, the camera's field of view was lit by three 760 nm wavelength LED lights; during the two other dives, the camera field was lit by two full spectrum white lights (wavelengths peak at 447 nm and 560 nm). A conductivity-temperature-depth (CTD) sonde (SeaBird SBE 49 FastCAT), an ADCP (Teledyne Navigator 1200 kHz), a Niskin bottle, and an internal computer were also mounted on the sled. The camera sled was connected to the ship via a steel standard armored fiber-optic cable that enabled real time data streaming at 10 Hz. Images were stored as a series of grayscale TIFF images.

The cameras faced horizontally into the water column for 26 of the 43 deployments; for the remaining 17 deployments, the cameras were pointed down towards the benthos. The primary focus of this study will be on the horizontal-looking dives where vertical profiles were taken (Table 1). Furthermore, only 18 of the 26 vertical deployments were analyzed due to either technical errors, procedural errors, or due to too much vertical movement caused by heave, which rendered the video unanalyzable. We sampled the water column from the surface to within 3 meters of the benthos, which ranged between 270 meters and 800 meters deep, except for the deployment at Palmer

Deep where the deepest depth sampled was 1300 meters. Deployment times varied between full light and full dark, with the majority of deployments having started between 9:00 and 21:00 EST.

Camera descent speeds were between 10 and 15 meters per minute and ascent speeds were between 30 and 50 meters per minute with data recorded continuously throughout the deployment. To observe and record the water column and organism abundance and behavior, camera rig descent was stopped every 50 meters for 1 to 2 minutes; these pauses will be referred to as horizons. If no identifiable krill were seen in the camera after 1 to 2 minutes at a horizon, the descent was resumed. If krill were present, the camera remained at the horizon between 2 and 10 minutes to record krill behavior.

2.2 Collection of Environmental Data

Environmental data were analyzed from two different sources: the camera sled CTD and shipboard surface data. Camera sled CTD physical data collected were temperature, depth, and salinity. Surface photosynthetically active radiation (PAR) was collected by the shipboard light sensors (Biospherical Licor Chelsea Sensor, Serial No. 4721).

Camera CTD salinity and temperature were used to create salinity and temperature profiles concurrent with filming. The camera mounted CTD failed on one of the deployments due to the freshwater rinse syringe remaining attached to the CTD. Furthermore, some unusually low shallow depth salinity values (< 33.5 ppt) were suspect and suggested the pre-deployment freshwater rinse of the CTD had frozen before the camera sled was put in the water.

Surface PAR data from the ship was utilized to determine daylight intensity and duration. To account for potential spikes which might have occurred during readings, the average of the highest 10% PAR values, or the maximum irradiance, was determined. The maximum irradiance for deployment times was used to determine if deployments occurred during light or dark. “Dark” is defined as PAR below $3 \mu\text{mol photons m}^{-2} \text{s}^{-1}$.

2.3 Identifying Parameters to Differentiate Krill from Particles

Two parameters were utilized to differentiate krill from non-krill: the aspect ratio, that is the major axis length divided by the minor axis length, and the pixel area of the object. Aspect ratio was used due to krill’s distinct body shape; krill have a much more elliptical shape than many marine particles, with most detritus having rounder, less elongated shapes. Area was chosen because, with very few exceptions, krill were the only organisms that came close to the cameras and were thus larger than most particles, and most detritus close to the camera were much smaller than krill close to the camera.

2.4 Image Filtering Method

Raw images were preprocessed to even compensate for the lighting pattern and to more easily differentiate krill from the water column. Three different preprocessing methods were tested. Filter 1 involved utilizing only a high-pass Gaussian filter to retain the krill but remove the broad lighting trend. Filter 2 involved using the Matlab built-in function `imadjust` to contrast stretch the image before utilizing the Gaussian filter. Filter 3 involved utilizing the built-in Matlab function `stretchlim` to alter the Matlab function `imadjust` to greatly increase pixel intensity contrasts before utilizing a Gaussian high-pass filter.

The accuracy of the three filters was tested using eight different segments of 600

images each, the equivalent of one minute of footage, representing different depths, abundances of krill, locations, and times of day (Table A.1). The images were processed using the three different filters before converting the images to binary. Krill blobs were identified using test values of 3.5 and 400 for aspect ratio and area, respectively. The number of krill were counted in every tenth image using both visual and algorithm methods; visual counts were made using the raw images, while algorithm counts were done using the processed binary images. This yielded a total of 480 images that were evaluated to compare visual counts of krill and non-krill objects to those identified automatically by the 3 different filters.

The statistical agreement between visual counts and corresponding algorithm counts was made using a Model II Regression. The regression coefficients and error estimates on the coefficients determine if a filter overestimated or underestimated the number of krill present in the footage. A Model II Regression was used because both visual and algorithm counts were made with error (i.e. both the dependent and independent variables were measured with error, Laws and Archie 1981). The slope, confidence intervals, R-values, and associated errors of the regression results were compared. Filter 3 was chosen for the subsequent analysis of all videos because the comparison between automated and visual counts yielded the greatest agreement, indicated by the greatest r-value, lowest error, and slope that reliably undersampled the abundance of krill, thus providing a conservative estimate of krill abundances (Table 2). Moreover, there were no extreme outliers observed with Filter 3, as was the case with Filter 1 and Filter 2 (Fig. A.2, Fig. A.3, Fig. A.4). We tested the krill yield of Filter 3 as a function of particle density and found no relationship between the number of krill seen

and the density of particles contaminating the images (Model II Regression, $R = -0.0737$, Fig. A.5). Thus, our estimates of krill abundances are not biased by the density of non-krill particles.

2.5 Parameter & Algorithm Assessment

After determining the filter scheme, the parameter values were adjusted to optimize the number of krill found, minimize the number of particles incorrectly identified as krill, and determine the overall accuracy of the algorithm. The aspect ratios and areas of known krill and non-krill blobs were collected from binary images and recorded. The number of krill identified and particles identified for different parameter values were plotted. Parameters were chosen based on their influence on the accuracy of the algorithm. An aspect ratio of 4 was determined to be sufficient to distinguish krill from non-krill particles; 58% of krill were identified, and the algorithm correctly identifies more krill than with other values (Fig. A.6, Fig. A.7). An area of 400 pixels was also determined to be satisfactory to identify krill and have few false-positives (Fig. A.8, Fig. A.9). Combining these two parameters and the associated errors, these values also ensure undersampling of the number of krill in the images.

2.6 Determination of Abundances of Krill

Krill abundances at all horizons were determined by averaging the number of krill seen over the number of images at each horizon (for how horizons were determined, see Appendix A.11). To account for potential avoidance of attraction of krill to the camera rig, the autocovariance of fluctuations in krill abundance in subsequent images at each horizon was determined. The first point where the autocovariance was equivalent to 0, which represents the point when the lagged time point varies randomly when compared

to the first time point selected, was used as the starting image for finding the average number and standard deviation of krill seen in the frames (Fig. A.12). This point was reached within 30 seconds for 75% of horizons, within 60 seconds for 95% of horizons, and within 120 seconds for all horizons. Due to initial fluctuations from camera attraction or avoidance, only video footage after abundances no longer co-varied were used to determine krill abundances; initial fluctuations were eliminated from the estimates of average abundance and variation therein.

To make deployments from different water columns comparable due to the range of bottom depths from the deployments, the absolute depth measurements were used to calculate relative depth, expressed as percent of total water column depth. Krill abundances at each horizon were matched with recorded environmental data from ancillary sensors through a common time stamp.

The Kruskal-Wallis test was used to determine differences between krill abundances at each horizon within each deployment. The Kolgomorov-Smirnov test was used to determine whether krill abundances using both absolute and relative depths, salinity profiles, or temperature profiles differed from each other. Differences were deemed statistically significant at $p < 0.05$.

Results

3.1 Camera System Assessment

The filters and parameters used to identify krill in the images were chosen to maximize the number of krill correctly identified in the images while minimizing the occurrence of errors. Filter 3, the filter which produced the greatest increase in the pixel intensity contrasts of the images before utilizing the Gaussian high-pass filter, was used due to the strong agreement between visually-identified and automatically-identified krill ($R^2 = 0.723$, $p < 0.001$, Table 2). Combining Filter 3 with a minimum aspect ratio of 4 and a minimum area of 400 pixels as parameters to distinguish krill from non-krill particles resulted in 69.2% of the algorithm-counted particles being krill; the algorithm accurately identifies 68.1% of the total krill visually identified. Combinations of filters and parameters with resulted in higher accuracies obtained lower krill abundances, while combinations that obtained higher krill abundances were less accurate and overestimated the abundance of krill (Fig. 1, Fig. 2)

3.2 Environmental Conditions

All salinity profiles followed the same trend, where salinity increased from between 33.9 ± 0.3 ppt at the surface to 34.5 ± 0.1 ppt at depths > 200 m (Fig. 3).

There were two general temperature profiles (Fig. 3). In Wilhelmina and Andvord Bay, the temperature increased from surface values of -0.8 ± 0.4 °C to 0.1 ± 0.2 °C around 150 meters before decreasing to -0.1 ± 0.2 °C at d. In Flandres Bay, the temperature slowly increased from around -1 °C at the surface to about 0.9 °C at depth, with the fastest increase in temperature occurring in the upper 100 meters.

Surface PAR values range from as low as $2 \mu\text{mol photons/m}^2\text{s}$ at night to as high

as 600 $\mu\text{mol photons/m}^2\text{s}$ during the day. The time between civil sunrise and sunset decreased over the course of the cruise from 6 hours 16 minutes to 3 hours 52 minutes. The average of the maximum irradiance for times during deployment ranged from 2 to 297 $\mu\text{mol photons/m}^2\text{s}$, representing ranges from full dark to bright, sunny days.

3.3 Krill Profiles

Krill in the three bays along the Western Antarctic Peninsula showed large spatial variability. Krill were found in 11 of the 18 deployments. In the profiles where krill were present, krill abundances were statistically different among depths within a profile (largest p-value < 0.001) and, among 8 of the 11 vertical profiles (largest p-value = 0.033). The remaining 3 deployments were statistically indistinguishable; the greatest krill abundance in these profiles was observed at the bottom of the profile. Krill were never seen above 100m, and the greatest abundances of krill in the vertical profiles consistently occurred at depths at or below 200 meters.

The vertical distributions of krill could be separated into two general profile types (Fig. 4). The first profile, Type I, was characterized by high abundances of krill present in the middle of the water column, between depths of 200 and 350 meters, or between 40% and 80% of the total depth of the deployment (Fig. 4A). Four profiles were characterized as Type I and were observed in Wilhelmina and Andvord Bay but not in Flandres Bay. The second profile, Type II, was characterized by peak abundances of krill found at the bottom of the water column at depths between 200m and 350m, equivalent to the lowest 20% of the water column for these deployments (Fig. 4B). Seven profiles were characterized as Type II and were observed in Andvord and Flandres Bay. The remaining seven deployments which contained no krill were categorized as Type 0 and

were observed in all bays.

The deployments were compared to one another based on profile type, salinity, temperature, and maximum surface irradiance at time of deployment. There was no relation found between krill abundances and either salinity or temperature. However, there appeared to be a correlation between profile type and maximum irradiance, although this relationship was not statistically significant ($p = 0.064$); all of Type I deployments occurred in the dark, while all but one of Type II deployments occurred during daylight (Fig. 5). Failure to observe krill occurred during both light and dark hours. During a 12-hour period where we sampled the same site, the depth of the maximum krill abundance changed by 150m, depending on if light was present or not (Fig. 6). Before dawn, a large abundance of krill was observed at 200m; after sunrise, the highest abundance was observed at 350m. After the sun set and light was no longer present, the largest abundance of krill was again observed at 200m.

Discussion:

Despite their key importance in Antarctic food webs and potential as sentinels of climate change, the abundance and distribution of Antarctic krill (*E. superba*) remain notoriously difficult to assess (Nicol 2006; Brierley 2008; Atkinson *et al.* 2012a, references therein). Here, we report *in situ* estimates of krill abundances and vertical distributions along the Western Antarctic Peninsula with a novel camera system. Utilizing this new system, we found peak krill abundances were either at midwater depths, generally when it was dark, or within a few tens of meters from the benthos, predominantly during the day.

Krill were never seen in waters shallower than 100m, and the highest abundances of krill were found at the benthos. Where krill are found in the water column during winter has been subject to some level of controversy. It is traditionally thought krill winter under sea ice in anticipation of the spring ice algal blooms (Hamner *et al.* 1983; Marschall 1988; Nicol 2006; Saba *et al.* 2014). However, biomass studies have found that there is not nearly enough space immediately under the sea ice cover to account for the total biomass found in summer (Lascara *et al.* 1999). Additionally, the concept of wintering under the sea ice is based on the notion that Antarctic krill are entirely pelagic and live in the upper 500 meters of the water column. Recent studies suggest adult Antarctic krill may utilize the full water column rather than the surface waters only and travel to the benthos regularly (Clarke and Tyler 2008; Schmidt *et al.* 2011; Atkinson *et al.* 2012a). Furthermore, the majority of krill biomass along the continental shelf of the Western Antarctic Peninsula can be found below 100 m in the open water column during winter and may be so deep as to not be detectable by sonar sampling (Lascara *et al.*

1999). Our findings show that krill are found at depth in winter, including depths below what ship sonars can typically sample.

There are several reasons why krill are likely to remain at depth during winter rather than migrating to the surface. One reason is where potential food resources are present. Phytoplankton are the preferential prey resource of krill (Haberman *et al.* 2003). However, there was a paucity of phytoplankton in the surface waters; the highest amount of Chl a in the bays sampled was less than 0.4 μ grams per liter, indicating very low phytoplankton abundance. Krill are known to frequently feed off the benthos (Clarke and Tyler 2008; Schmidt *et al.* 2011; Cleary *et al.* 2012). Given the low concentration of phytoplankton in the water column, our observation that krill were preferentially found deeper and in greatest numbers near the benthos indicates that these aggregations are responding to localized prey sources associated with the benthos.

Remaining at depth may also decrease krill metabolic rates. Krill are exposed to very little to no irradiance at depth. In previous studies, the metabolic rates of krill in complete darkness decrease significantly compared to krill exposed to light (Teschke *et al.* 2007). Studies have also shown that, under simulated winter conditions, krill consume significantly less food than during summer conditions, even when exposed to high abundances of food (Atkinson *et al.* 2002; Teschke *et al.* 2007). This reduced prey intake may be because krill must utilize energy to digest prey (Ikeda and Dixon 1984), and reduced prey intake may be indicative of an energy reduction strategy during winter. Our observations of krill distributions may not only be driven by potential prey exposure, but rather as an adaptive strategy to lower metabolic costs and prolong survival under food-limited conditions.

Additionally, we observed a correlation between the presence of light and krill profile type; greater krill abundances at depth during the day and greater krill abundances shallower in the water column at night. These changes in the depth of the maximum krill abundance could be attributed to diel vertical migration behavior. The diel vertical migration of Antarctic krill is a well-documented phenomenon that is attributed to predator-avoidance behavior, where krill avoid sight predators during the day by remaining at depth and come up at night to feed (Lascara *et al.* 1999; Nicol 2006; Atkinson *et al.* 2012a). Krill may migrate towards the benthos during the day to hide from baleen whales, one of their main predators (Quentin and Ross 1991). Baleen whales are abundant in the bays in the Western Antarctic Peninsula during the winter (Nowacek *et al.* 2011); whales were observed most days during our field season. However, the depths at which large krill abundances were found in our study precluded any sight predators and thus eliminated that hypothesis. Furthermore, Nowacek *et al.* (2011) also observed greater Humpback whale foraging at night, when krill were found at depths whales could dive to, than during the day. Our observations of the changes in the depth of the maximum krill abundance do not support winter krill vertical movements being motivated by anti-predatory behavior.

A more likely reason krill may continue to exhibit diel vertical migration during winter conditions is due to their circadian rhythm. As in most zooplankton, the primary cue of Antarctic krill diel vertical migration is considered to be changes in irradiance (Haney 1988; Ringelberk 1995). However, we observed krill at depths generally considered too deep for them to perceive changes in surface irradiance (Hiller-Adams and Case 1984). Light may not be the only zeitgeber maintaining the daily vertical

migrations (Gaten *et al.* 2008). Numerous laboratory and *in situ* studies have shown that zooplankton likely have an endogenous rhythm which contributes to consistent diel vertical migrations even when light cues are absent (Haney 1988; Velsch and Champalbert 1994; Gaten *et al.* 2008). Also, Mazzotta *et al.* (2010) discovered Antarctic krill have a *cryptochrome* gene which, as in many other organisms, influences and helps maintain their endogenous biological cycle. As krill were not found above 100 meters, and high abundances never above 200 meters, it is most likely that an endogenous circadian rhythm, rather than environmental changes in irradiance, maintain the vertical migration of Antarctic krill during the winter.

As is typical with most sampling instruments, we identified several limitations of the krill camera system. One such constraint is the effective field of view. The effective depth of field of view of the camera system was limited to 1-3 meters in front of the camera. Part of the limited depth of field is caused by the red lights used to illuminate the water column; 760 nm wavelengths are absorbed quickly by water, often within the first meter or so. However, we used the red light to avoid visually stimulating and attracting krill. Also, while the camera system can observe multiple krill individuals at one time, it cannot be used to observe an entire swarm. Krill swarms can be very large, with usually at least one dimension ranging from tens of meters to thousands of meters long (Tarling *et al.* 2009; Cox *et al.* 2010). The limited field of view of the camera system means krill within a swarm can be observed, but the extent of the entire swarm cannot.

Even with these limitations, there are many advantages to using the stereo camera system. Stereo camera systems are relatively non-invasive and are thought to not startle

krill (Letessier *et al.* 2013). We accounted for camera effects on krill abundances through eliminating observations, typically in the first minute of the video, that were indicative of correlated krill densities, rather than temporally independent estimates. The accuracy of krill individuals identified by our algorithm is comparable to field image studies of the Video Plankton Recorder (Davis *et al.* 2004; Hu and Davis 2005). Additionally, using accurate algorithms to identify organisms from thousands of images means data can be processed much more quickly than manually identifying organisms (Hu and Davis 2005), and this system can provide considerably higher spatial and temporal resolution. Ultimately, this automated approach can deliver a highly resolved estimate of the spatial and temporal abundance of krill and variations therein.

A major advantage of the camera system is that it can be used to observe krill throughout the water column, including close to the benthos. This system can be used to estimate krill abundances deeper in the water column than traditional sonar methods. Sonar systems are a non-invasive way to study krill swarms in the upper 500m of the water column and observe large-scale krill distributions (Zhou and Dorland 2004; Atkinson *et al.* 2012a, references therein). The krill camera system is capable of observing krill vertical distributions as deep as 2000 meters. Ultimately, the camera system introduced here provides much smaller-scale estimates of krill abundances but does so in regions of the water column that are inaccessible to some other methods.

The krill camera system will enable the study of the full habitat of the krill and not just the surface waters. Most estimates of krill biomass are based on surface water sampling done during the summer and limiting krill habitat to the upper 400m of the water column; however, Schmidt *et al.* (2011) estimates up to 20% of the summer krill

population may reside deeper than 400 m. Krill may be a source of iron for phytoplankton in the summer from their benthic diet (Schmidt *et al.* 2011). In winter, krill are not a source of iron, since they do not migrate to the surface waters, indicating a weakening or even a reversal of benthic-pelagic coupling. The distance of krill diel vertical migration is measured to be 100m (Godlewska 1996); this is again based on estimates from only part of krill habitat. A larger diel vertical migration distance could mean that krill are capable of reintroducing more nutrients from the benthos to surface waters than previous estimates. Studying the full vertical distributions of krill will enable a better understanding of how krill impact the vertical transfer of energy and matter in the Southern Ocean.

Overall, utilization of this stereo camera system has provided a unique opportunity to use a non-invasive system to quantify krill distributions in remote areas during the poorly-studied winter season. Our findings show that krill undergo very limited vertical movements and reside at depth rather than surface waters in winter. This implies a weakening in the benthic-pelagic coupling caused by krill movements, as they have limited interactions with surface waters. Furthermore, we found that krill abundances were greater in the middle of the water column at night and higher at the benthos during the day; this may indicate krill continue daily vertical migrations in winter, but the stimulus for this vertical movement is likely light-independent. The krill camera system enabled *in situ* observations of the small-scale spatial heterogeneity of Antarctic krill and quick, accurate processing of the images from deployments. Using the camera system in conjunction with traditional net tows and sonar transects will provide more robust sampling and ultimately more accurate estimates of krill *in situ* behaviors

and abundances. These estimates are critical to understanding the pivotal role this keystone species plays in the Southern Ocean food webs and how they might respond to a warming climate in the Western Antarctic Peninsula region.

Figures and Tables:**Table 1. Deployment Number, Date, Time, Lat., Long, and Location of the 18 Krill**

Camera Deployments. The times are in EST, local time. The latitudes and longitudes are given within each of the 3 bays where deployments occurred. Depth refers to the maximum depth of the water column during the deployment

Dive Number	Date	Time (EST)	Lat.	Long.	Location	Depth
3	20-May-13	9:12	64°40.944 S	62°13.877 W	Wilhelmina	500 m
5	21-May-13	14:03	64°32.097 S	62°14.062 W	Wilhelmina	600 m
6	21-May-13	19:00	64°32.097 S	62°14.063 W	Wilhelmina	600 m
9	23-May-13	15:20	64°50.790 S	62°36.844 W	Andvord	277 m
11	24-May-13	13:39	64°48.257 S	62°43.340 W	Andvord	300 m
14	25-May-13	1:19	64°48.788 S	62°42.107 W	Andvord	374 m
15	25-May-13	6:53	64°48.501 S	62°43.023 W	Andvord	341 m
16	25-May-13	13:19	64°48.629 S	62°43.048 W	Andvord	352 m
17	25-May-13	19:11	64°48.698 S	62°42.271 W	Andvord	343 m
18	26-May-13	16:32	64°48.594 S	62°43.009 W	Andvord	344 m
20	27-May-13	10:54	64°48.596 S	62°43.003 W	Andvord	347 m
24	29-May-13	13:43	65°02.956 S	63°18.757 W	Flanders	243 m
25	29-May-13	14:56	65°02.955 S	63°18.758 W	Flanders	200 m
26	29-May-13	16:34	65°02.992 S	63°18.886 W	Flanders	269 m
29	30-May-13	12:38	65°01.264 S	63°15.527 W	Flanders	510 m
31	30-May-13	19:53	65°01.262 S	63°15.512 W	Flanders	517 m
38	4-Jun-13	18:22	64°37.113 S	62°14.317 W	Wilhelmina	499 m
39	4-Jun-13	20:11	64°37.096 S	62°14.301 W	Wilhelmina	497 m

Table 2. Results of Model II Regression to compare visual and algorithm counts on sample videos using 3 distinct filters. Filter 3 has the highest R values, the lowest errors, and the smallest confidence interval and was used for all subsequent analysis.

	Filter 1	Filter 2	Filter 3
Slope	0.506	1.356	0.563
Y-Intercept	-0.766	-4.798	0.693
95% Confidence Intervals	0.469	1.241	0.537
	0.543	1.471	0.590
Difference btw Confidence Intervals	0.074	0.230	0.053
F	229.086	51.532	1266.100
Total degrees of freedom	487	487	487
Probability of observing F	0	0	0
R ²	0.320	0.096	0.723
R-value	0.566	0.310	0.851
Adjusted R ²	0.319	0.094	0.722
Standard Regression Error	3.431	11.603	2.247
Standard Slope Error	0.019	0.059	0.014

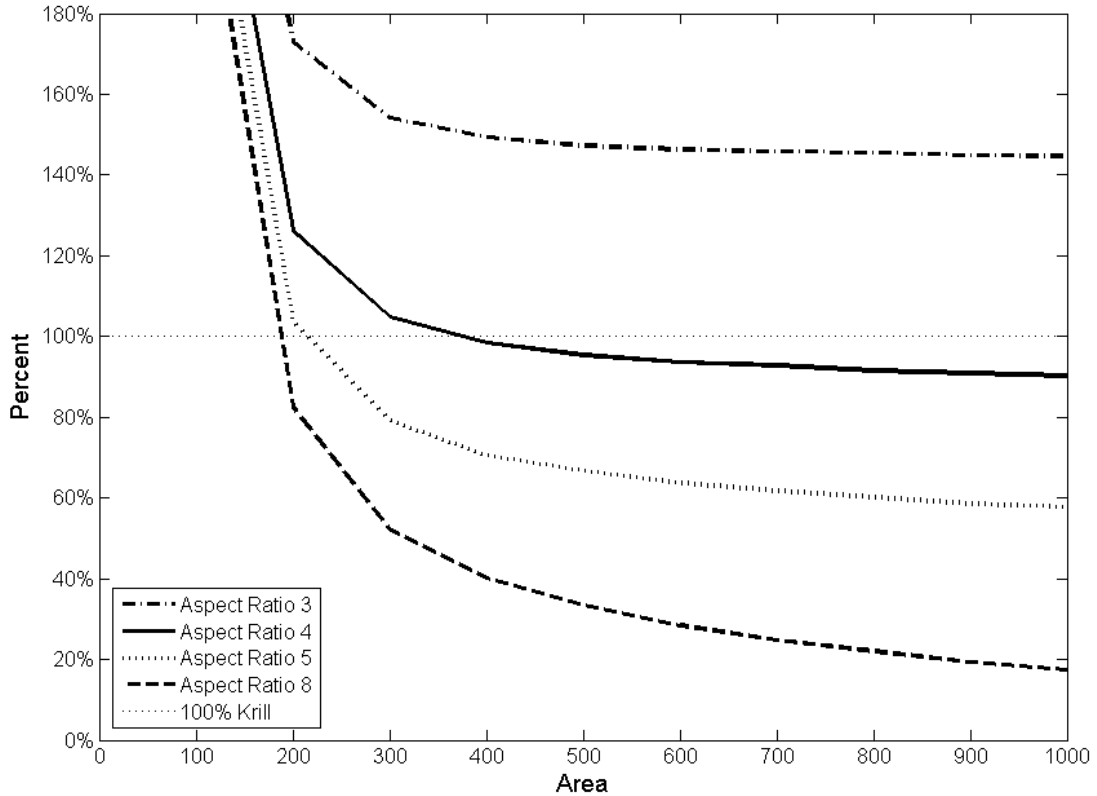


Figure 1. The Percentage of the Number of Particles Identified as Krill by the Algorithm to the Visual Count of Krill (y-axis) when using different parameter values (different Area values on the x-axis, different Aspect Ratio values represented by different lines). Ideally, the algorithm should undersample the number of krill seen in the images (below the thin dotted line). There is a trend where, the larger the values of the aspect ratio or area, the fewer particles are identified as krill by the algorithm. Parameter values should be strict enough to obtain relatively accurate krill identification, yet slack enough to capture larger yields of krill. Using an aspect ratio value of 4 and an area of 400 means the number of particles identified as krill are close to, yet still under, the number of krill visually identified.

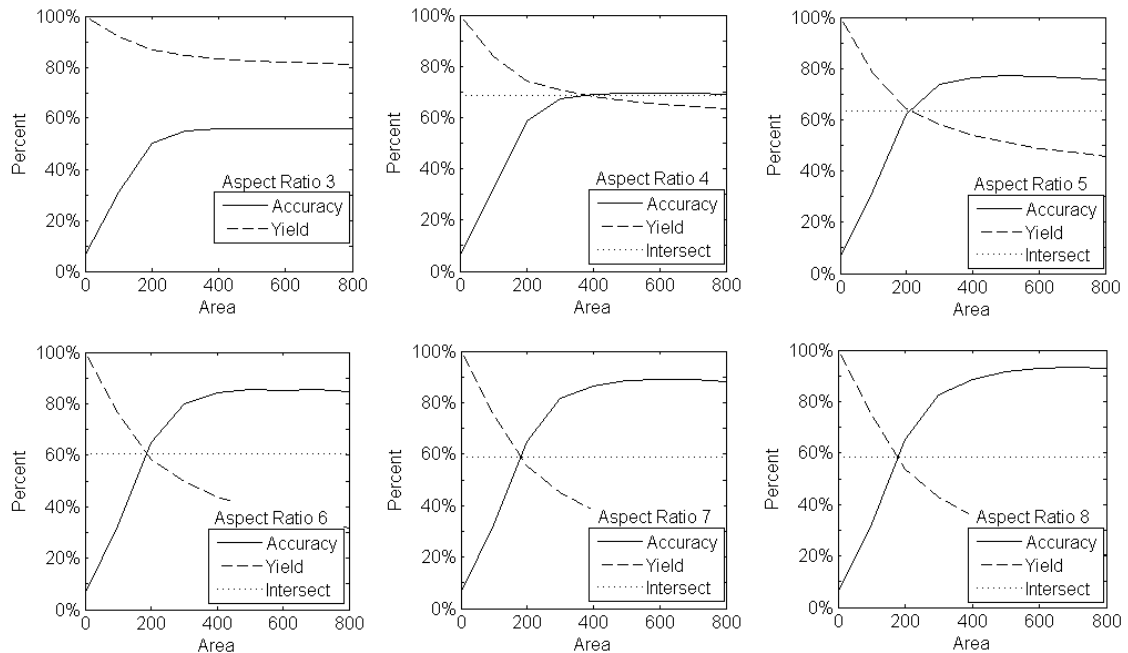


Figure 2. Comparison of Accuracy and Yield of Parameter Values of Algorithms.

Each graph represents the percentage of the total krill identified (accuracy - solid line) and the percentage of blobs correctly-identified as krill (yield - dashed line) of the algorithm when different aspect ratio and area values are used. Changes in area are represented on the x-axis, percentages are on the y-axis, and the different graphs represent different aspect ratio values from 3 to 8. In general, the greater the aspect ratio and area, the greater the accuracy. However, as the aspect ratio and area values increase, the algorithm identifies fewer krill. The dotted black line shows where the two lines intersect, or where the accuracy of the algorithm is similar to the amount of krill obtained. For aspect ratio of 3, the two lines never intersect; the accuracy remains lower than the amount of krill identified. For Aspect Ratio 4, it intersects at about 68.8%; for Aspect Ratio 5, at 63.5%; for Aspect Ratio 6, at 60.7%; and for Aspect Ratio 7, at about 59.0%. As the point where the accuracy of the algorithm and the amount of krill obtained

is highest at an Aspect Ratio of 4, and this point occurs around an Area of 400, these were the finalized values of the algorithm.

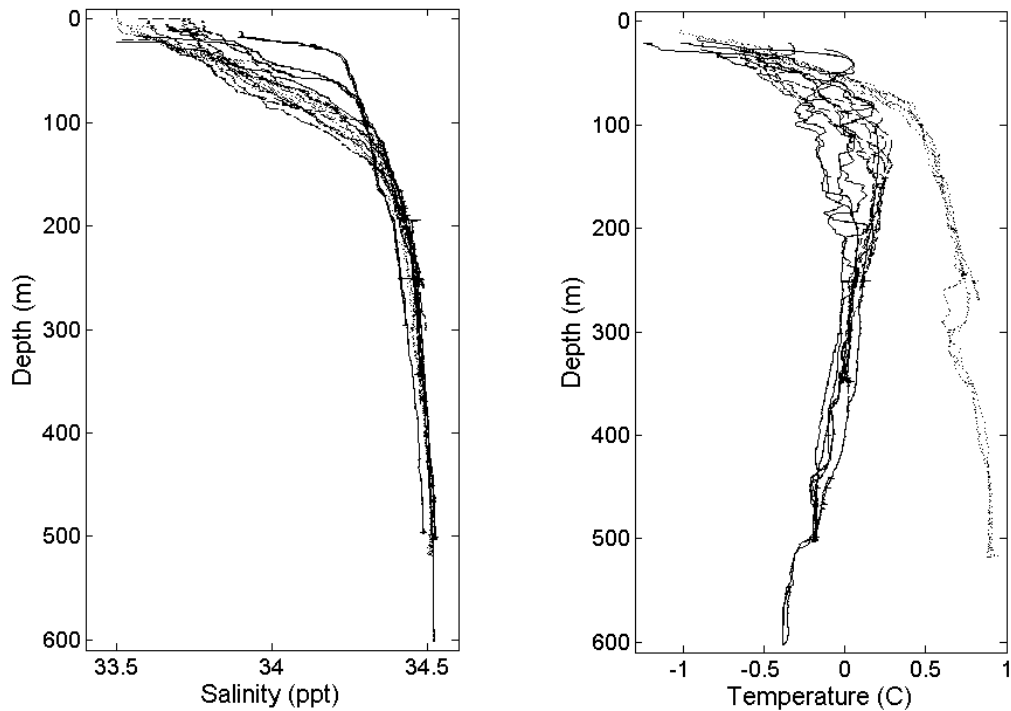


Figure 3. Salinity (left) and temperature (right) profiles for vertical profile deployments. Deployment locations are distinguished by line: solid lines are from Wilhelmina Bay, dashed lines are from Andvord Bay, and dotted lines are from Flanders Bay. (*Left*) Depth is in meters along the y-axis, salinity is parts per thousand along the x-axis. Salinities in general ranged about 1ppt between 33.5 ppt and 34.5 ppt. (*Right*) Depth is in meters along the y-axis, temperature in °C along the x-axis. Two distinct profiles were evident, with Wilhelmina and Andvord Bay increasing to 0°C before decreasing with depth, and Flanders Bay temperatures increasing with depth. Temperatures range in Wilhelmina and Andvord Bays by 1°C and in Flanders Bay by about 2°C.

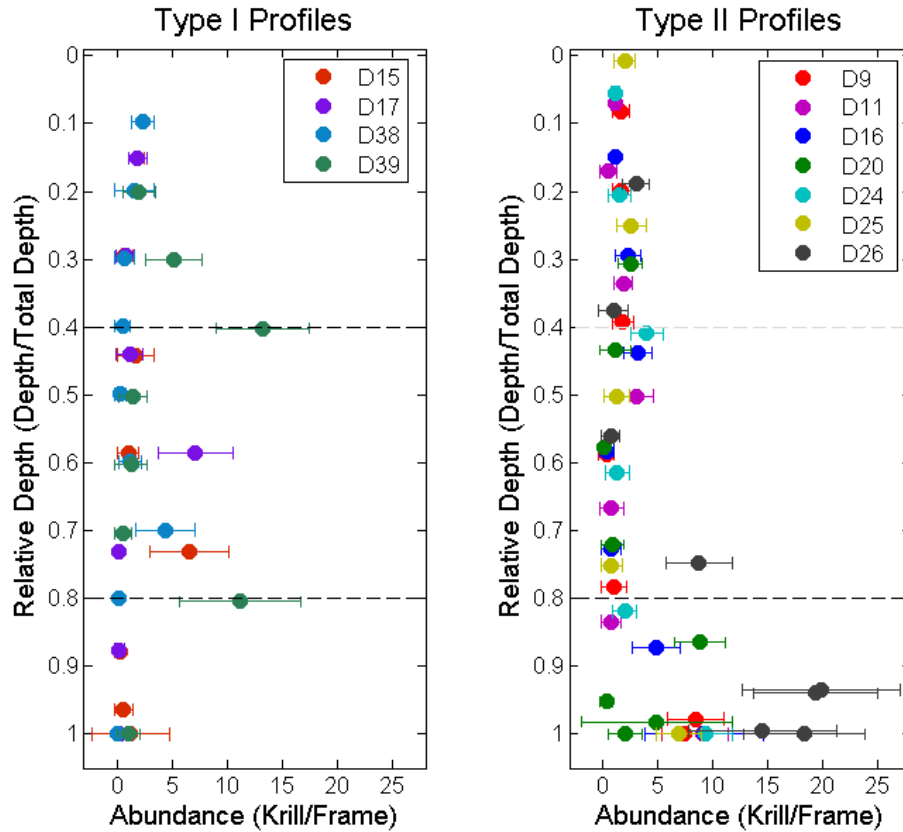


Figure 4. Profiles of Krill Distributions. A profile was characterized as Type I if the depth with the highest abundance of krill was between 40% and 80% of the relative water column depth (left); the area between the black dotted lines represents the depth in the water column between 40% and 80%. A profile was characterized as Type II if the depth with the highest abundance was in the bottom 20% of the water column (right). The bottom 20% of the water column is below the black dotted line.

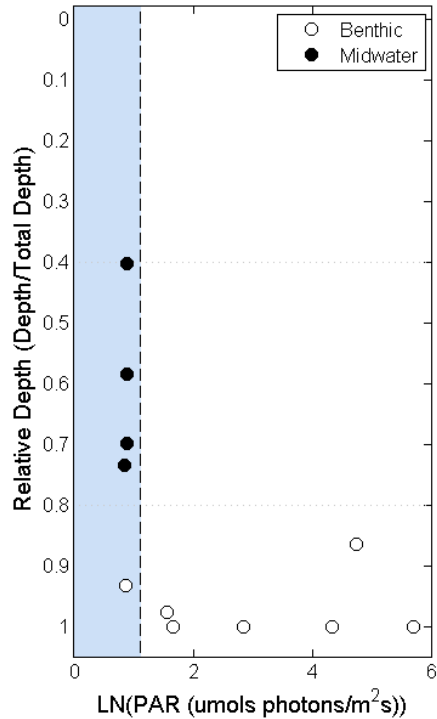


Figure 5. PAR at Time of Deployment to Relative Depth of Maximum Krill

Abundance. Relative depth, from surface (0) to bottom (1), where maximum krill abundance was found (y-axis) versus maximum irradiance of deployment (x-axis). The relative depths of the maximum krill abundance of Type I (Midwater) profiles is represented by the dark circles, while the relative depths of the maximum krill abundance of Type II (Benthic) profiles is represented by the open circles. The dashed line represents the cutoff between light and dark; deployments occurring in the shaded region occurred at night, while deployments occurring in the non-shaded region occurred during the day.

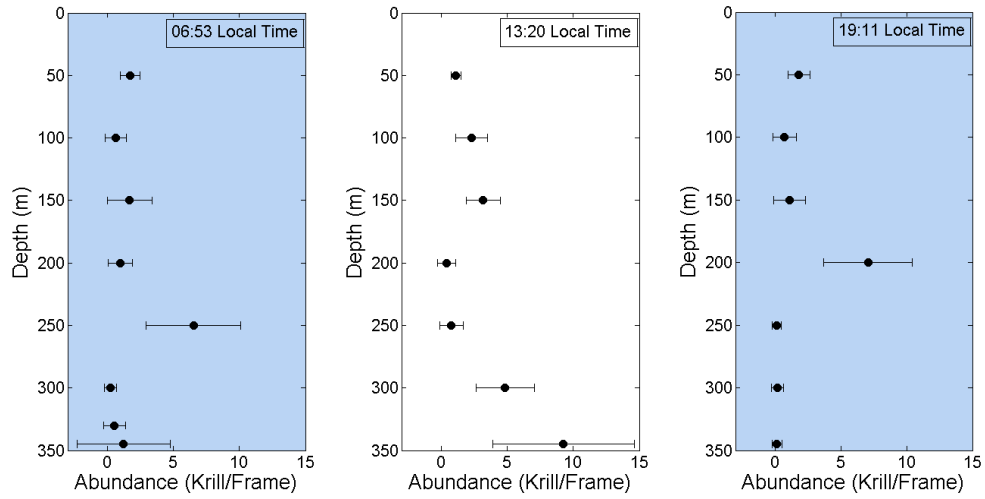
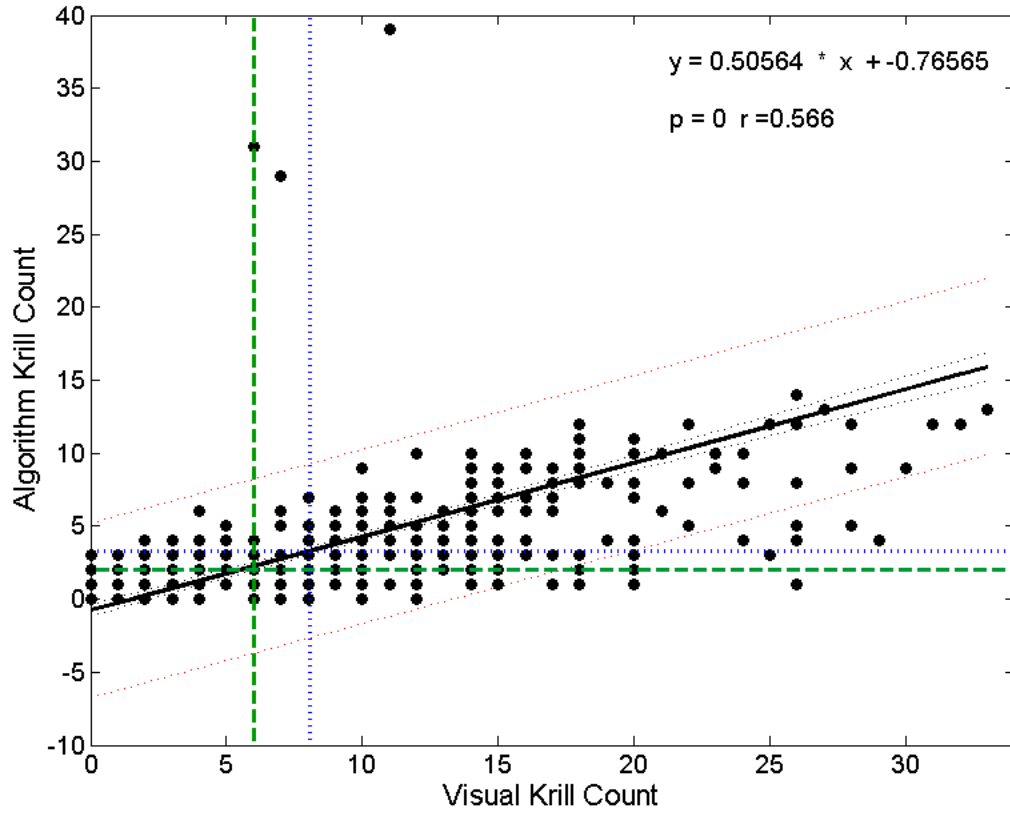


Figure 6. Changes in the vertical distribution of krill over three consecutive deployments at the same station. The shaded plots (left and right) represent deployments which occurred under “dark” conditions; the unshaded graph (middle) occurred when light was present.

Thesis Appendix

Table A.1. Details of Test Horizon Images: the date, time, and depth of the images used to test the filtering schemes. Each segment was comprised of six hundred images starting from the times listed above. The test images all had different abundances of krill, including a deployment horizon where no krill were present (Deployment 31).

Deployment	Date	Time	Horizon Depth
3	5/20/2013	14:49 UTC	465 m
4	5/20/2013	23:28 UTC	250 m
15	5/25/2013	11:07 UTC	150 m
17	5/25/2013	23:34 UTC	200 m
20	5/27/2013	15:27 UTC	250 m
25	5/29/2013	19:26 UTC	200 m
26	5/29/2013	21:03 UTC	200 m
31	5/31/2013	00:19 UTC	200 m



Filter A.2. Visual krill count (x-axis) versus algorithm krill counts (y-axis) and model II regression best-fit line (solid black) and confidence intervals (red lines) for Filter 1. The dotted green lines cross at the median of the data (median (6,2)), and the blue dotted lines cross at the mean values (mean (8, 3)).

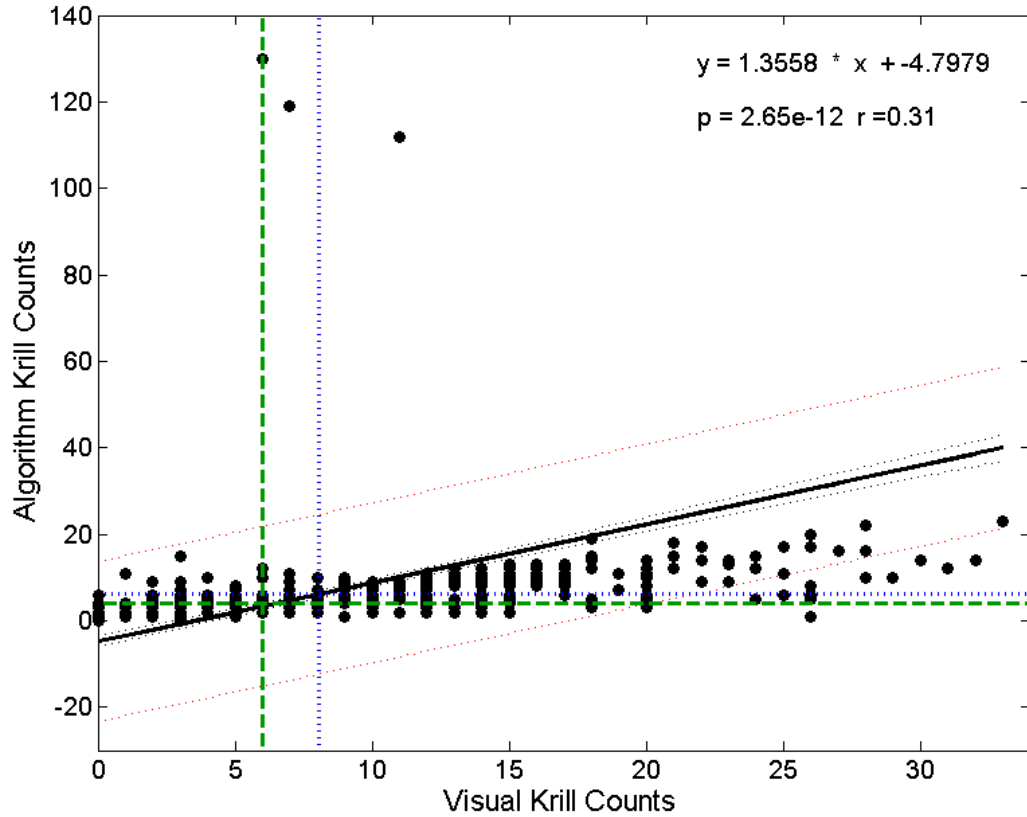


Figure A.3. Visual krill count (x-axis) versus algorithm krill counts (y-axis) and model II regression best-fit line (black) with confidence intervals (red lines) for Filter 2. The dotted green lines cross at the median of the data (median (6,4)), and the blue dotted lines cross at the mean values (mean (8, 6)). There are three outliers which are an order of magnitude higher than any of the other krill counts.

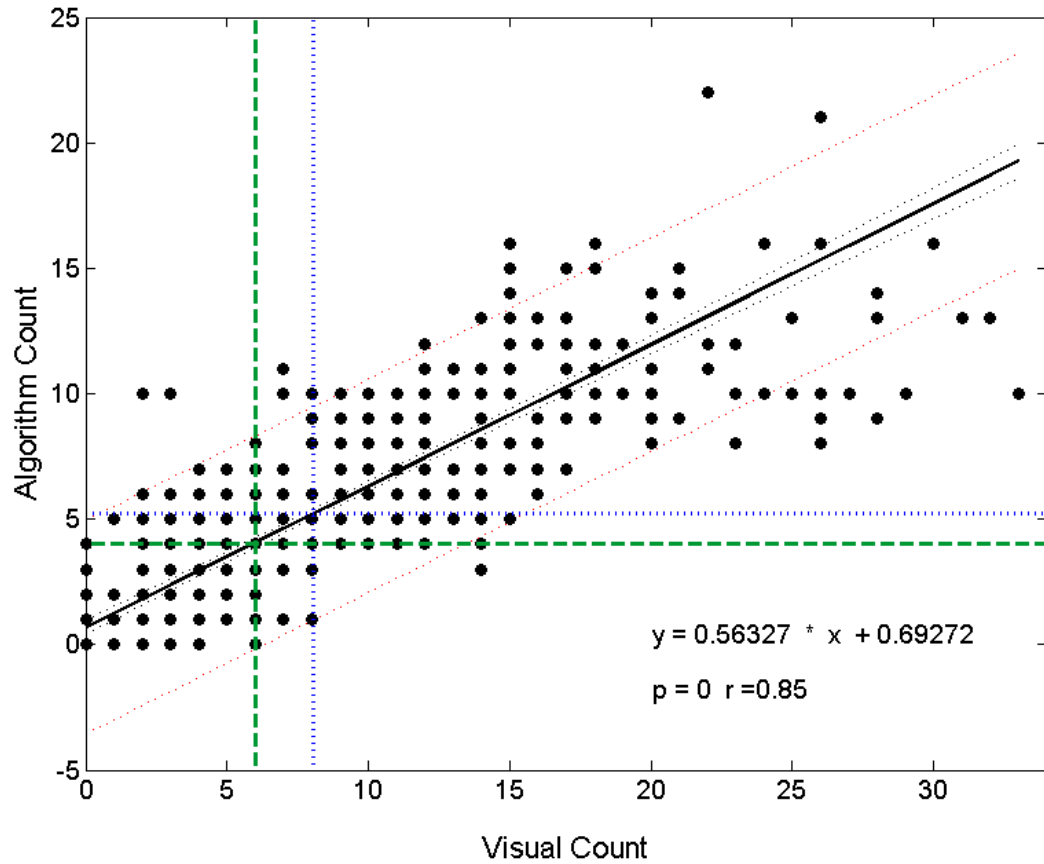


Figure A.4. Visual krill count (x-axis) versus algorithm krill counts (y-axis) and model II regression best-fit line (solid black) and confidence intervals (red) for Filter 3. The dotted green lines cross at the median of the data (median (6,4)), and the blue dotted lines cross at the mean values (mean (8, 5)). There are no extreme outliers when this filter is used.

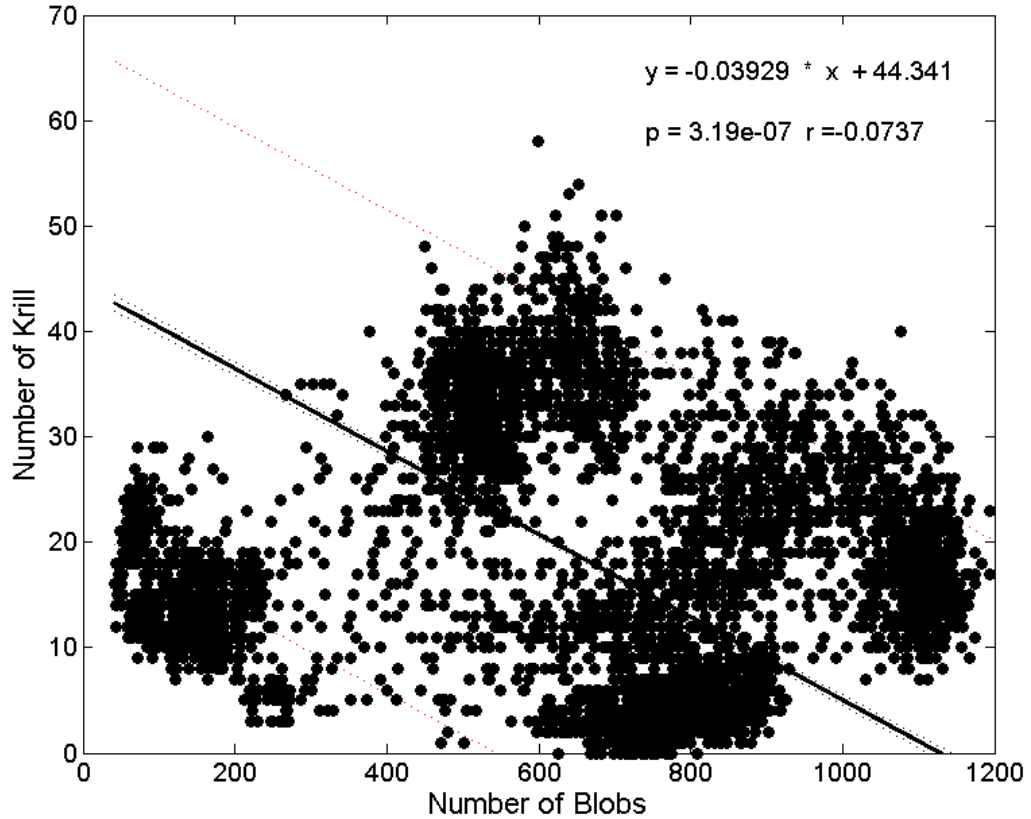


Figure A.5. Comparison of the number of blobs in an image (x-axis) to the number of krill identified (y-axis). This is for the Filter 3 and showed the least correlation between the number of blobs and the number of krill identified. There is very little relation between the number of blobs and the number of krill found, as evidenced by the low r value.

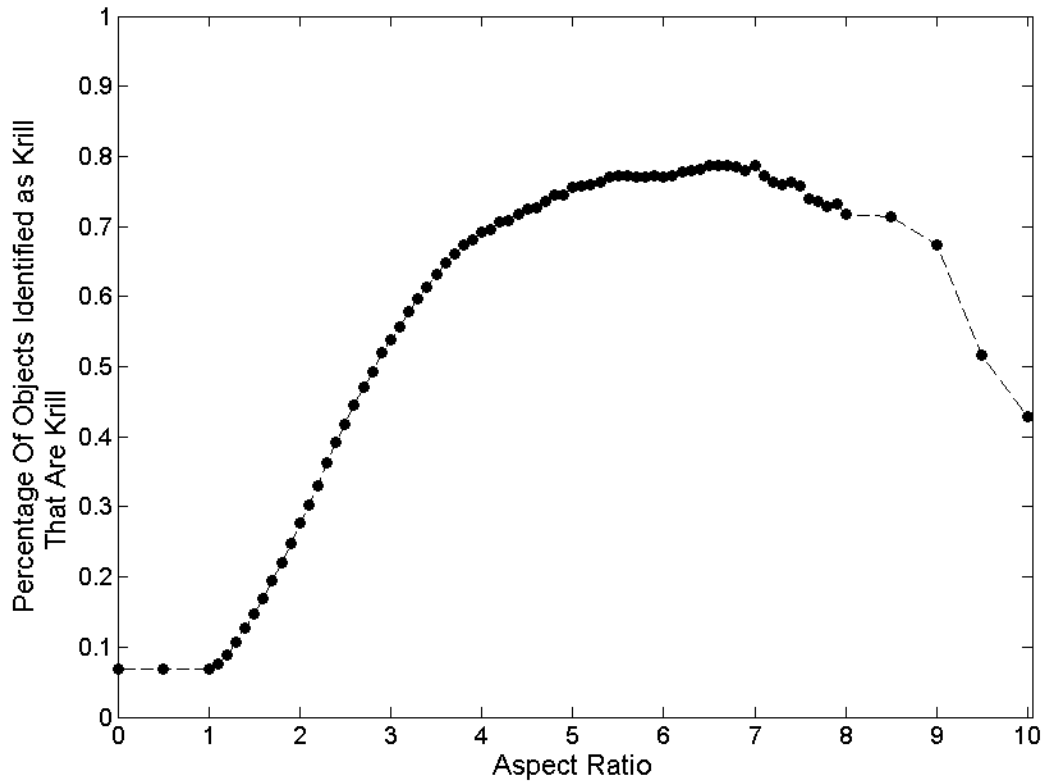


Figure A.6. The percent composition of objects identified as krill based on Aspect Ratio value (ratio of major axis to minor axis). The percentages represent the percentage of objects correctly identified as krill when using the specific Aspect Ratio value. At an aspect ratio of 4, there is a greater than 50% chance that an object will be correctly identified as a krill.

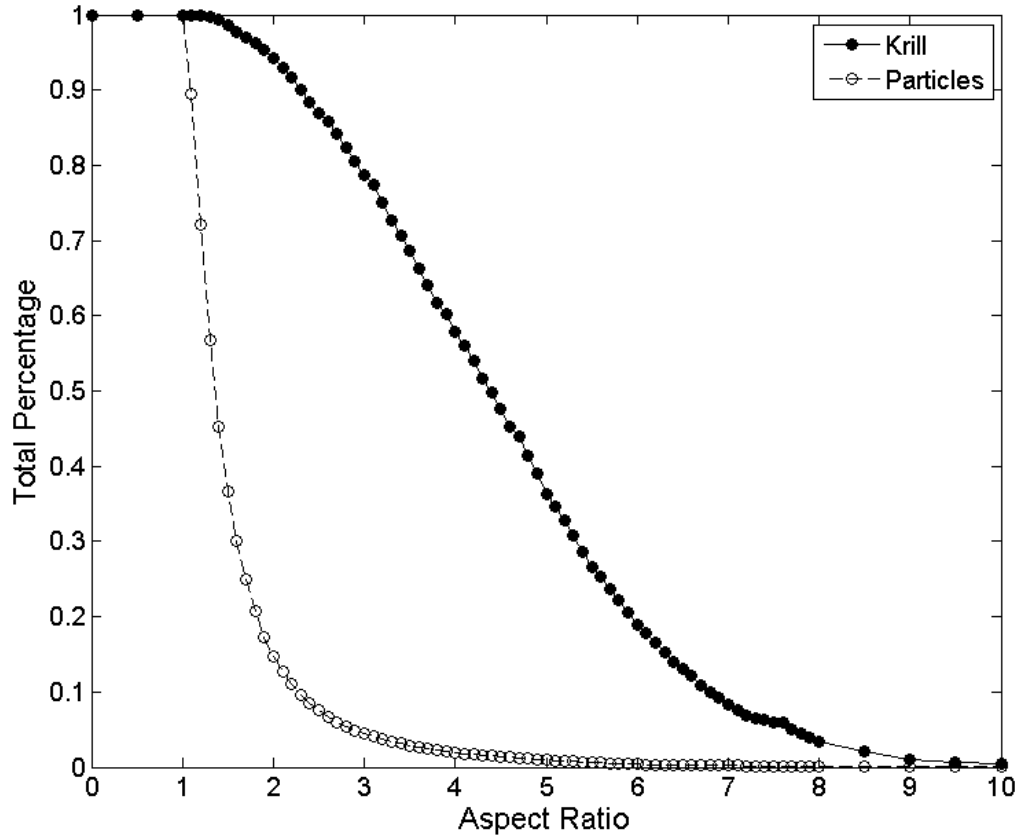


Figure A.7. Percentage of objects (open circles) and krill (closed circles) which are identified as krill by the algorithm based on different aspect ratios. At the aspect ratio of 3, the number of particles incorrectly identified as krill tapers off. The number of particles are completely minimized around the aspect ratio of 6.5. Using an aspect ratio of 4, the number of incorrectly-identified particles is minimized and the number of correctly-identified krill is maximized.

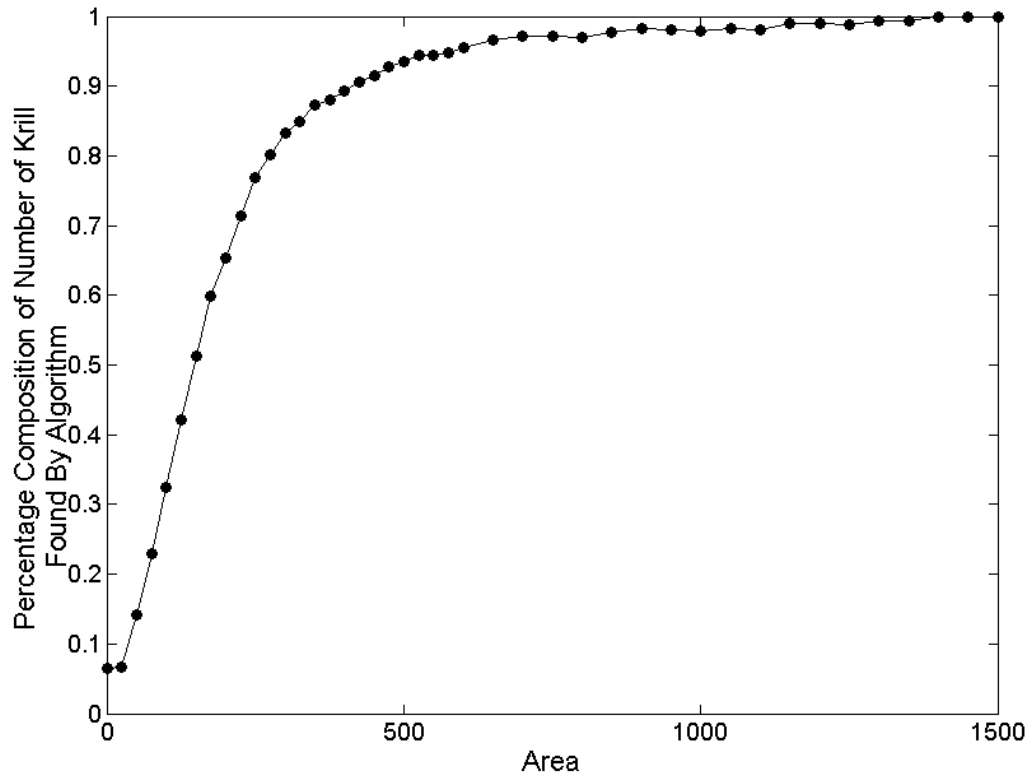


Figure A.8. Percent composition of the number of krill identified by the algorithm and labeled as krill according to different blob area sizes. The percentage of correctly-identified krill increases with greater area due to marine particles being much smaller than krill close to the camera.

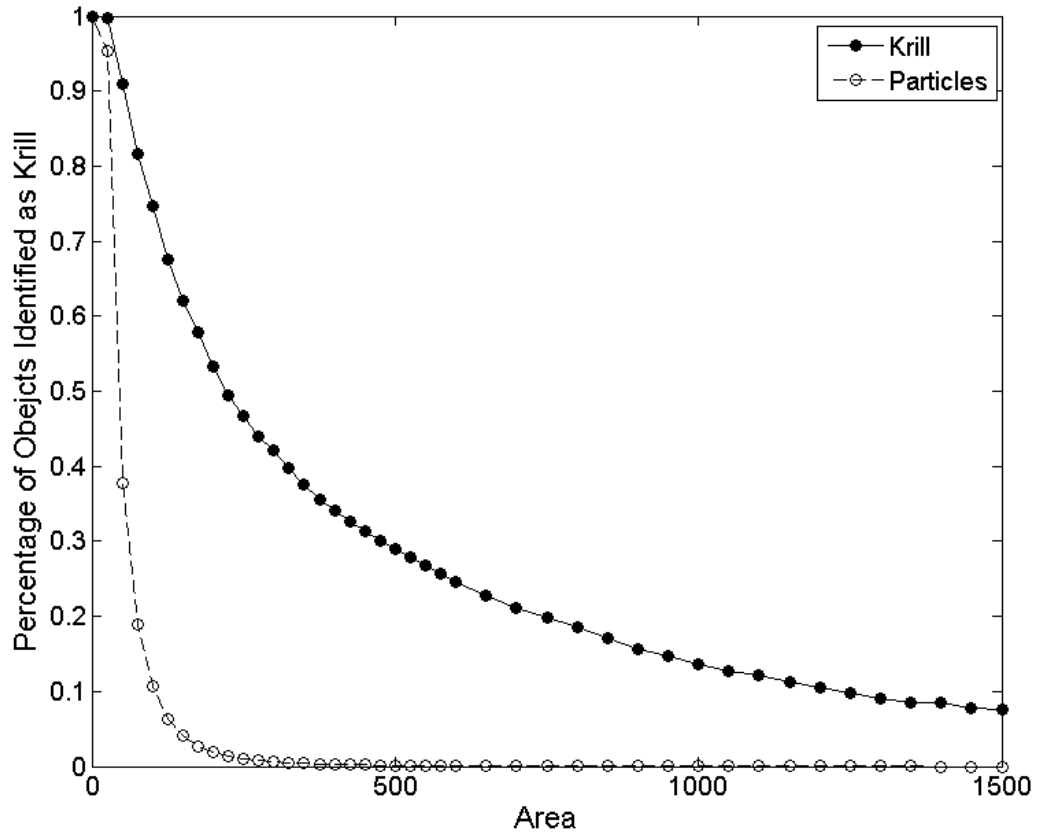


Figure A.9. Percentage of objects (open circles) or krill (closed circles) identified by different blob areas. As the threshold area for blobs to be identified as krill increases, the percentage identified as krill decreases. At an area of 200 pixels, the percentage of particles incorrectly identified as krill is limited. At an area of 400 pixels, the percentage of particles erroneously identified as krill is very small.

A.10 Horizon Determination

Horizons were determined using the depth and time data from the CTD attached to the camera sled. Potential horizons were determined to be areas where the depth difference within 1.3 seconds was less than 0.05 meters; descent was assumed to have resumed when the distance within 1.3 seconds was greater than 0.05 meters. Because images were saved with time stamps, the horizon images could be determined as the images between the start time of a horizon and the end time of a horizon. Horizons were further defined as having more than 300 images; if a horizon had less than 300 images, it was assumed to be a glitch and not included in the profiles. This prevented accidental horizons where the camera movement was slowed by the heave of the ship.

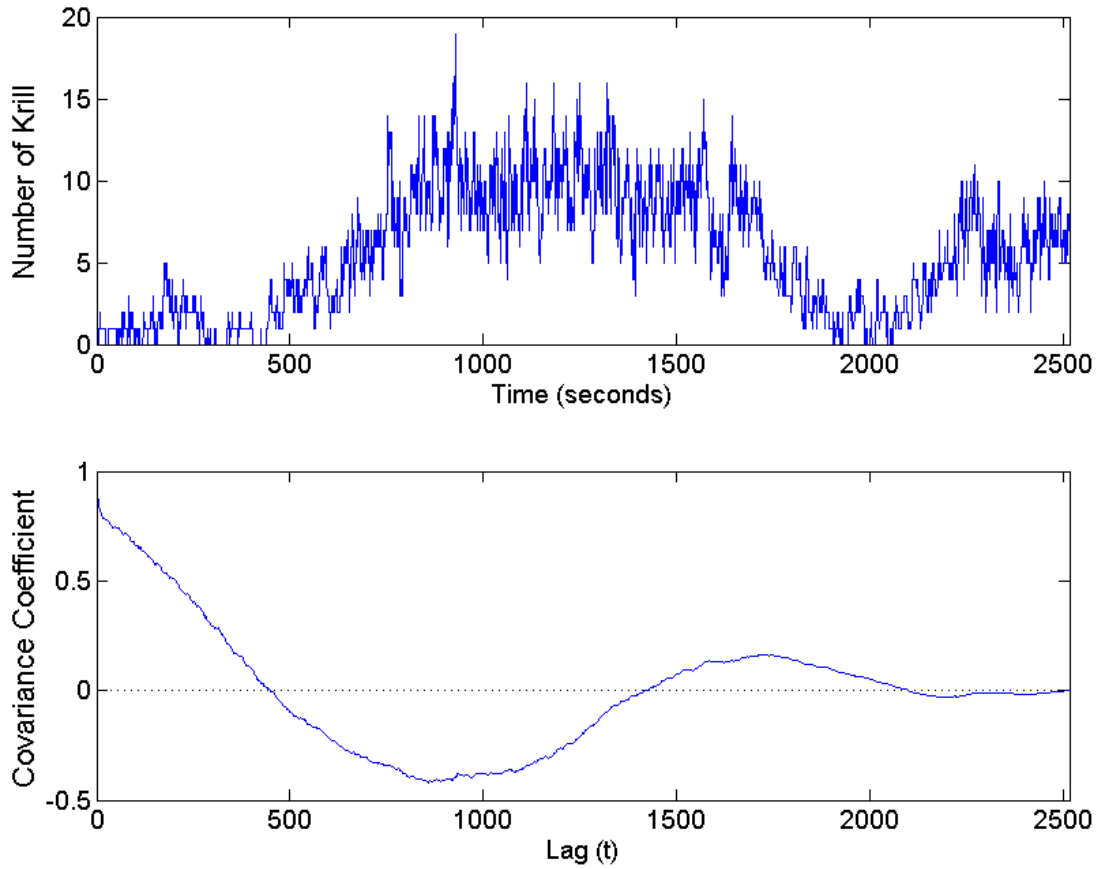


Figure A.11. Plots showing (top) the raw number of krill seen over time and (bottom) the covariance plotted against lag time. The average number of krill per frame at this horizon started from image 448, where the covariance crosses from positive to negative, to the end of the horizon, to the last image at the horizon. All other krill averages were found using the same method.

References:

- Ashjian, C.J., C.S. Davis, S.M. Gallagher, P.H. Wiebe, and G.L. Lawson. 2008. Distribution of larval krill and zooplankton in association with hydrography in Marguerite Bay, Antarctic Peninsula, in austral fall and winter 2001 described using the Video Plankton Recorder. *Deep Sea Research II* **55**: 455-471
- Atkinson, A., B. Meyer, D. Stübing, W. Hagen, K. Schmidt, *et al.* 2002. Feeding and energy budgets of Antarctic krill *Euphausia superba* at the onset of winter – II. Juveniles and adults. *Limnol. Oceanogr.* **47(4)**: 953-966
- Atkinson, A., V. Siegel, E.A. Pakhomov, M.J. Jessopp, and B. Loeb. 2009. A re-appraisal of the total biomass and annual production of Antarctic krill. *Deep-Sea Research I* **56**: 727-740. doi: 10.1016/j.dsr.2008.12.007
- Atkinson, A., S. Nicol, S. Kawaguchi, E. Pakhomov, L. Quentin, *et al.* 2012a. Fitting *Euphausia superba* into Southern Ocean Food-Web Models: a review of data sources and their limitations. *CCAMLR Science* **19**: 219-245
- Atkinson, A., K. Schmidt, S. Fielding, S. Kawaguchi, and P.A. Geissler. 2012b. Variable food absorption by Antarctic krill: Relationships between diet, egestion rate and the consumption and sinking rates of their fecal pellets. *Deep-Sea Research II* **59-60**: 147-158. doi: 10.1016/j.dsr2.2011.06.008
- Benfield, M.C., P.H. Wiebe, T.K. Stanton, C.S. Davis, S.M. Gallagher, *et al.* 1998. Estimating the spatial distribution of zooplankton biomass by combining Video Plankton Recorder and single-frequency acoustic data. *Deep-Sea Research II* **45**: 1175-1199

- Brierley, A.S. 2008. Antarctic Ecosystem: Are Deep Krill Ecological Outliers or Portents of a Paradigm Shift? *Current Biology* **18(6)**: 252-254
- Clarke, A., and P.A. Tyler. 2008. Adult Antarctic Krill Feeding at Abyssal Depths. *Current Biology* **18**: 282-285. doi: 10.1016/j.cub.2008.01.059
- Cleary, A.C., E.G. Durbin, and T.A. Ryneerson. 2012. Krill feeding on sediment in the Gulf of Maine (North Atlantic). *Mar Ecol Prog Ser* **455**: 157-172. doi: 10.3354/meps09632
- Cox, M.J., J.D. Warren, D.A. Demer, G.R. Cutter, and A.S. Brierley. 2010. Three-dimensional observations of swarms of Antarctic krill (*Euphausia superba*) made using a multi-beam echosounder. *Deep-Sea Research II* **57**: 508-518
- Cresswell, K.A., G.A. Tarling, S.E. Thorpe, M.T. Burrows, J. Wiedenmann, *et al.* 2009. Diel vertical migration of Antarctic krill (*Euphausia superba*) is flexible during advection across the Scotia Sea. *J. Plankton Res.* **31(10)**: 1265-1281
- Davis, C.S., Q. Hu, S.M. Gallager, X. Tang, & C.J. Ashjian. 2004. Real-time visualization of plankton abundance and taxonomic composition using the Video Plankton Recorder. *Deep-Sea Research II* **43**: 1947-1970
- De Robertis, A. 2002. Size-dependent visual predation risk and the timing of vertical migration: an optimization model. *Limnol. Oceanogr.* **47**: 925-933
- Gaten, E., G. Tarling, H. Dowse, C. Kyriacou, and E. Rosato. 2008. Is vertical migration in Antarctic krill (*Euphausia superba*) influenced by an underlying circadian rhythm? *Journal of Genetics* **87(5)**: 473-483
- Godlewska, M. 1996. Vertical migrations of krill (*Euphausia superba* Dana). *Pol. Arch. Hydrobiol.* **14**: 9-63

- Haberman, K.L., R.M. Ross, and L.B. Quentin. 2003. Diet of Antarctic krill (*Euphausia superba* Dana): II. Selective grazing in mixed phytoplankton assemblages. *Journal of Experimental Marine Biology and Ecology* **283**: 97-113
- Hagen, W., E.S. Van Vleet, and G. Kattner. 1996. Seasonal lipid storage as overwintering strategy of Antarctic krill. *Mar Ecol Prog Ser* **134**: 85-89
- Hamner, W.M., P.P. Hamner, S.W. Strand, and R.W. Gilmer. 1983. Behavior of Antarctic Krill, *Euphausia superba*: Chemoreception, Feeding, Schooling, and Molting. *Science (Washington, D.C.)* **220**: 433-435
- Haney, J.F. 1988. Diel Patterns of Zooplankton Behavior. *Bulletin of Marine Science* **43(3)**: 583-603
- Hiller-Adams, P. and J.F. Case. 1984. Optical parameters of euphausiid eyes as a function of habitat depth. *Journal of Comparative Physiology A* **154**: 307-318
- Hu, Q., and C. Davis. 2005. Automatic plankton image recognition with co-occurrence matrices and Support Vector Machine. *Mar Ecol Prog Ser* **295**: 21-31143-
- Ikeda, T. and P. Dixon. 1982. Body shrinkage as a possible overwintering mechanism of the Antarctic krill, *Euphausia superba* Dana. *Journal of Experimental Marine Biology and Ecology* **62**: 143-151
- Ikeda, T., and P. Dixon. 1984. The Influence of Feeding on the Metabolic Activity of Antarctic Krill (*Euphausia superba* Dana). *Polar Biol* **3**: 1-9
- Kawaguchi, K., O. Matsuda, S. Ishikawa, and Y. Naito. 1986. A Light Trap to Collect Krill and Other Micronektonic and Planktonic Animals Under the Antarctic Coastal Fast Ice. *Polar Biology* **6**: 37-42

- Kawaguchi, S., R. Kilpatrick, L. Roberts, R.A. King, and S. Nicol. 2011. Ocean-bottom krill sex. *Journal of Plankton Research*. doi:10.1093/plankt/fbr006
- Lascara, C.M., E.E. Hofmann, R.M. Ross, and L.B. Quetin. 1999. Seasonal variability in the distribution of Antarctic krill, *Euphausia superba*, west of the Antarctic Peninsula. *Deep-Sea Research I* **46**: 951-984
- Laws, E.A., and J.W. Archie. 1981. Appropriate use of regression analysis in marine biology. *Marine Biology* **65**: 13-16
- Le Fèvre, J., L. Legendre, R.B. Rivkin. 1998. Fluxes of biogenic carbon in the Southern Ocean: roles of large microphagous zooplankton. *Journal of Marine Systems* **17**: 325-345
- Letessier, T.B., S. Kawaguchi, R. King, J.J. Meeuwig, R. Harcourt, *et al.* 2013. A Robust and Economical Underwater Stereo Video System to Observe Antarctic Krill (*Euphausia superba*). *Open Journal of Marine Science* **3**: 148-153. doi: 10.4236/ojms.2013.33016
- Marschall, H.P. 1988. The Overwintering Strategy of Antarctic Krill Under the Pack-Ice of the Weddell Sea. *Polar Bio.* **9**: 129-135
- Mazzotta, G.M., C. De Pittà, C. Benna, S.C.E. Tosatto, G. Lanfranchi, *et al.* 2010. A *CRY* From the Krill. *Chronobiology International* **27(3)**: 425-445
- Menden-Deuer, S., and D. Grünbaum. 2006. Individual Foraging Behaviors and Population Distributions of a Planktonic Predator Aggregating to Phytoplankton Thin Layers. *Limnol. Oceanogr.* **51(1)**: 109-116
- Nicol, S. 2006. Krill, Currents, and Sea Ice: *Euphausia superba* and Its Changing Environment. *BioScience* **56(2)**: 111-120

- Nicol, S., and A.S. Brieley. 2010. Through a glass less darkly – New approaches for studying the distribution, abundance and biology of Euphausiids. *Deep-Sea Research II* **57**: 496-507. doi :10.1016/j.dsr2.2009.10.002
- Nowacek, D.P., A.S. Friedlaender, P.N. Halpin, E.L. Hazen, D.W. Johnston, *et al.* 2011. Super-Aggregations of Krill and Humpback Whales in Wilhelmina Bay, Antarctic Peninsula. *PLoS ONE* **6(4)**: e19173. doi: 10.1371/journal.pone.0019173
- Quentin, L.B., and R.M. Ross. 1991. Behavioral and Physiological Characteristics of the Antarctic Krill, *Euphausia superba*. *Amer. Zool.* **31**: 49-63
- Ringelberg, J. 1995. Changes in light intensity and diel vertical migration: a comparison of marine and freshwater environments. *J. Mar. Biol. Ass. U.K.* **75**: 15-25
- Saba, G.K., W.R. Fraser, V.S. Saba, R.A. Iannuzzi, K.E. Coleman, *et al.* 2014. Winter and spring controls on the summer food web of the coastal West Antarctic Peninsula. *Nature Communications.* **5**:4318 doi: 10.1038/ncomms5318
- Schmidt, K., A. Atkinson, S. Steigenberger, S. Fielding, M.C.M. Lindsay, *et al.* 2011. Seabed foraging by Antarctic krill: Implications for stock assessment, benthopelagic coupling, and the vertical transfer of iron. *Limnol. Oceanogr.* **56(4)**: 1411-1428. doi: 10.4319/lo.2011.56.4.0000
- Tarling, G.A., T. Klevjer, S. Fielding, J. Watkins, A. Atkinson, *et al.* 2009. Variability and predictability of Antarctic krill swarm structure. *Deep-Sea Research I* **56**: 1994-2012
- Teschke M., S. Kawaguchi, and B. Meyer. 2007. Simulated light regimes affect feeding and metabolism of Antarctic krill, *Euphausia superba*. *Limnol. Oceanogr.* **52(3)**: 1046-1054

- Torres, J.J., J. Donnelly, T.L. Hopkins, T.M. Lancraft, A.V. Aarset, *et al.* 1994.
Proximate composition and overwintering strategies of Antarctic micronektonic crustacea. *Marine Ecological Progress Series* **113**: 221-232
- Velsch, J.P., and G. Champalbert. 1994. Swimming activity rhythms in *Meganyctiphanes norvegica*. *C. R. Acad. Sci. Paris Sci. Vie* **317**: 857-862
- Wiebe, P.H., C.J. Ashjian, S.M. Gallager, C.S. Davis, G.L. Lawson, *et al.* 2004. Using a high-powered strobe light to increase the catch of Antarctic krill. *Marine Biology* **144**: 493-502
- Zhou, M., and R. D. Dorland. 2004. Aggregation and vertical migration behavior of *Euphausia superba*. *Deep-Sea Research II* **51**: 2119-2137
- Zhou, M., W. Nordhausen, and M.E. Huntley. 1994. ADCP measurements of the distribution and abundance of euphausiids near the Antarctic Peninsula in winter. *Deep Sea Research I* **41**: 1425-1445